Journal of Environmental Informatics Letters 7(2) 80-89 (2022)

Journal of Environmental Informatics Letters

www.iseis.org/jeil

Analysis of Transport Channel and Pollution Source Area of Atmospheric Particulate Matter in Beijing, China Based on Hybrid Single-Particle Lagrangian Integrated Trajectory Model

J. Chen[1] and C. Y. Zhou[1 *]

[1] *North China Electric Power University, Beijing 102206, China*

Received 07 May 2022; revised 25 May 2022; accepted 01 June 2022; published online 28 June 2022

ABSTRACT. Regional air pollution is affected not only by local pollution emissions but also by the trans-regional transportation of pollutants in adjacent areas. To explore the potential contribution source area of atmospheric particulate matter affecting Beijing, based on the Global Data Assimilation System of the National Centers for Environmental Prediction (December 2016 ~ November 2021), this study uses the Hybrid Single-Particle Lagrangian Integrated Trajectory model to cluster the 72-hour backward airflow trajectory arriving in Beijing by season. Combined with the ground observation data of $PM_{2.5}$ and PM_{10} mass concentration, the spatial characteristics of different traffic routes in Beijing and their contribution to the accumulation of $PM_{2.5}$ and PM_{10} concentration are analyzed by using the Potential Source Contribution Function and the Concentration Weighted Trajectory, which provides a reasonable theoretical basis for the coordinated treatment of regional air pollution. The results show that the distribution of potential contribution source areas of $PM_{2.5}$ and PM_{10} in Beijing has obvious seasonal characteristics, and the concentration contribution of different transportation routes is significantly different. In winter, the distribution of potential source areas shows a trend from northwest to Southeast, which forms a conveyor belt from central Inner Mongolia of China to Beijing through Zhangjiakou of Hebei Province. The high concentration contribution areas of $PM_{2.5}$ and PM_{10} are concentrated in the urban area of Beijing, Baoding of Hebei Province, and the west of Tianjin. In spring and autumn, the potential source areas are distributed from south to north, which mainly cover the central part of Hebei Province and the urban area of Beijing. The high concentration contribution areas of $PM_{2.5}$ and PM_{10} are smaller than those in winter, and are dotted in Baoding, Shijiazhuang and other places of Hebei Province.

Keywords: atmospheric particulate matter, backward trajectory mode, Beijing, cluster analysis, concentration weighted trajectory, potential contribution source area, potential source contribution function

1. Introduction

Since the second industrial revolution, the global industry has developed rapidly. At the same time, the environmental pollution caused by industrial production has become increasingly prominent. The pollution of the atmospheric environment has caused great climate change, global warming, and the hole in the ozone hole, which threatens people's daily life. Especially the particles discharged into the atmosphere are inhaled into the human body, causing chronic respiratory and cardiovascular diseases, and seriously affecting human health (Yue et al., 2020; Geng et al., 2021). Due to the fluidity of the atmosphere, the regional air pollution is related not only to the local emission sources, but also to the distant pollution sources (Zheng et al., 2019). In the study of the air pollution process, the analysis of pollutant source area/source can provide a positive theoretical basis and suggestions for regional collabrative control of atmospheric particulate matter emission pollution (PEY et al., 2009; Zhang et al., 2017).

The main methods to study the regional transport of pollutants are the pollution path method (Zhu et al., 2010; Balachandran et al., 2013), the Lagrange particle diffusion model method (Zhao et al., 2020), and the particle source tracing method (Marcazzan et al., 2001; Chen et al., 2016). The backward trajectory pollution path method has significant advantages in reducing errors and the interpretability of pollutant transport (Salvador et al., 2010). Many researchers have conducted abundant research on regional air pollution using the HYSPLIT backward trajectory model, including the discussion on the potential source area and contribution rate of pollutants (Dimitriou, 2015; Do et al., 2015; Qian et al., 2018; Wang et al., 2020; Li et al., 2022), the research on the characteristics of pollution transport at different levels and heights (Wang et al., 2016; Du et al., 2018; Tu et al., 2019), and quantifying the contribution value of local and foreign sources in the period of heavy pollution (Tiwari et al., 2012; He et al., 2018; Guo et al., 2021). However, the literature mentioned above mostly focuses on the specific application of a specific time or a trajectory analysis method, does not systematically analyze the differences in pollutant transport characteristics and potential source areas in different seasons, and

[*] Corresponding author. Tel.: 86-13810430880.
E-mail address: zhouchangyu@ncepu.edu.cn (C. Y. Zhou).

ISSN: 2663-6859 print/2663-6867 online
 doi:10.3808/jeil.202200081

lacks the overall analysis of the spatial distribution characteristics of potential source areas of regional air pollutants.

Based on the five-year atmospheric particle concentration detection data and NCEP reanalysis meteorological data in Beijing from 2016 to 2021, this study uses the HYSPLIT model, Potential Source Contribution Function (PSCF), and Concentration-weighted Trajectory (CWT) analysis methods to gradually analyze the transport path, transport process and distribution characteristics of potential source areas of pollutants in Beijing in four seasons, and quantitatively analyze the transport contribution of different regions, provinces, and cities. The research results can provide a scientific basis for the prevention and control of air pollution in Beijing. It also has certain significance for the coordinated prevention and control of air pollution between adjacent cities.

2. Data and Methodolgogy

2.1. Overview of the Study Area

Beijing is an area located at the northern end of the North China Plain, adjacent to the Bohai Bay, with mountains in the northwest and plains in the southeast. The climate of Beijing is a typical warm temperate semi-humid continental monsoon climate, with short spring and autumn; In summer, affected by the southeast ocean airflow, it is hot and rainy. In winter, it is mainly affected by the cold air in Siberia, and the climate is cold and dry. The complex changes in meteorological conditions make the concentration of atmospheric particulate matter in Beijing have significant seasonal differences. In addition, as the economic center of northern China, Beijing has dense cities and towns and developed industries in the southern plains. The West and north of Beijing are Taihang Mountains and Yanshan Mountains, and the impact of human activities is relatively small. This geographical pattern also has a certain impact on the distribution of pollution source areas. Relatively speaking, the change in meteorological conditions is more complex, and the law of human activities will not change much in a short time, which makes the source area of air pollution more obviously affected by meteorological changes.

2.2. Methodology

In this study, the coordinates of central Beijing are selected as the receiving point for the study of airflow trajectories. Firstly, cluster analysis is carried out on the airflow trajectories passing through the receiving point in different seasons to explore the source of the airflow trajectories of the receiving point in different seasons, and the impact of the concentration of air pollutants carried by different trajectories on the atmospheric environment in Beijing is analyzed. Then, this study conducts PSCF and CWT analysis on all airflow trajectories acting on the receiving point, and quantitatively studies the regional spatial distribution and weight concentration of potential source contribution of different regions to the receiving point. Finally, the influence of different meteorological conditions in different seasons on the concentrations of $PM_{2.5}$ and PM_{10} in Beijing was studied by using the Spearman correlation analysis method.

2.3. HYSPLIT Model

HYSPLIT model is a professional model for calculating and analyzing the transport and diffusion trajectories of air pollutants jointly developed by the Air Resources Laboratory of the National Oceanic and Atmospheric Administration (NOAA) and the Australian Meteorological Administration (Draxler et al., 1998; Stein et al., 2015; Draxler et al., 2017). The model has a relatively complete transport, diffusion, and sedimentation model to deal with a variety of meteorological element input fields, a variety of physical processes, and different types of pollutant emission sources.

2.4. Cluster Analysis

Backward trajectory clustering is to cluster a large number of airflow trajectories according to the moving speed, path space area, and moving direction of air mass trajectories, to sort out the trajectories with the closest spatial similarity for classification. Since this study mainly researches the direction of the airflow trajectory reaching the receiving point, the algorithm in this study adopts the angle clustering method in transit (Borge et al., 2007; Wang et al., 2009), turns the research area into a $0.1° \times 0.1°$ horizontal grid, and clusters and groups the air mass trajectories of all the receiving point areas of the arrival mode by calculating the spatial change of the combination of each two airflow trajectories.

2.5. Potential Source Contribution Function

PSCF can solve the location of the potential source area through the combination of the backward trajectory of airflow and some element value (such as mass concentration of $PM_{2.5}$). The function of this method is based on spatial grid calculation, which is defined as the ratio of the number of contaminated airflow trajectory ends passing through a grid in the study area to the number of all airflow trajectory ends passing through the grid.

In this paper, the secondary standard limits of the daily average values of $PM_{2.5}$ and PM_{10} (75 and 150 $\mu g \cdot m^{-3}$) are taken as the criteria to determine whether the trajectory is polluted or not, that is, when the pollutant concentration corresponding to the air mass trajectory passing through a grid reaches Beijing exceeds the secondary standard limit, the trajectory is a pollution trajectory, on the contrary, it is a clean trajectory. The high-value grid area is considered to be the potential source area of atmospheric particulate matter in Beijing.

The value of PSCF is a conditional probability. When the overall stagnation time of the trajectory of some remote grids is less, the analysis result has great uncertainty. Therefore, the weight factor (W_{ij}) is introduced to reduce the probability of the grid. When the number of tracks passed by a grid is less than three times the average number of track endpoints in each grid in the selected research area, W_{ij} is used to reduce the uncertainty of PSCF results (Ashbauch et al., 1985; Tian et al., 2016):

$$PSCF_{i,j} = \frac{m_{i,j}}{n_{i,j}} \qquad (1)$$

$$WPSCF = W_{ij} \cdot PSCF_{ij} \quad (2)$$

where $m_{i,j}$ is the number of pollution tracks passing through the grid (i, j), $n_{i,j}$ is the number of all tracks passing through the grid (i, j), and W_{ij} is defined as follows:

$$W_{ij} = \begin{cases} 1.00, & 80 \le n_{ij} \\ 0.70, & 20 < n_{ij} < 80 \\ 0.42, & 10 < n_{ij} < 20 \\ 0.05, & 0 < n_{ij} < 10 \end{cases} \quad (3)$$

2.6. Concentration-Weighted Trajectory

PCSF has limitations in reflecting the grid pollution tracking. When the pollutant concentration is higher than the set standard, the weight of the grid unit can be the same, which can not well reflect the pollution degree of the pollution tracking (Liu et al., 2013). Therefore, the weighted concentration of the trajectory is calculated by CWT to make up for this deficiency, and the method can quantitatively give the average weighted concentration of each grid and reflect the pollution degree of different trajectories (Seibert, 1994). The specific methods are as follows:

$$C_{ij} = \frac{1}{\sum_{l=1}^{M} \tau_{ijl}} \sum_{l=1}^{M} C_l \tau_{ijl} \quad (4)$$

where C_{ij} is the average weight concentration of the cell grid (i,j). l is the trajectory. M is the total number of tracks. C_l is the corresponding pollutant mass concentration when the trajectory passes through the grid (i,j). τ_{ijl} is the dwell time of the trajectory l on the grid (i,j). The same weighting factor as PSCF is adopted to reduce the uncertainty of the C_{ij}, as follows:

$$WCWT = C_{ij} \times W_{ij} \quad (5)$$

2.7. Data Source

The airflow trajectory data from December 1, 2016 to November 30, 2021 used in this study are from the Global Data Assimilation System (GDAS) meteorological data of the National Environmental Prediction Center (NECP) (ftp://arlftp.arlhq.noaa.gov/pub/archives/gdas1). The hourly mass concentration data of $PM_{2.5}$ and PM_{10} are from the observed mean values of 8 national control points of the Beijing Environmental Protection Testing Center. The experimental study simulates a backward trajectory point every 6 hours with a time scale of 72 hours, which can not only reflect the characteristics of cross-regional transport of air pollutants but also cover the life cycle of secondary pollutants. The simulation height of the experiment is 500 meters, which can not only represent the regional characteristics of near-ground wind flow and reaction airflow but also reduce the influence of near-ground friction.

3. Results and Discussion

3.1. Backward Trajectory Cluster Analysis

To reveal the differences in airflow trajectories in Beijing in different seasons, this study makes a cluster analysis of hourly backward trajectories in the Beijing urban areas from December 2016 to November 2021. According to the climate characteristics of Beijing, the month is divided into four seasons: winter (December to February), spring (March to May), summer (June to August), and autumn (September to January). The airflow trajectories of the four seasons are clustered into 4 clusters, 7 clusters, 3 clusters, and 4 clusters. The clustering results of airflow trajectories in each season are shown in Figure 1.

In winter, most of the airflows come from the west and northwest. The northwest airflow tracks 1 and 2 from Siberia

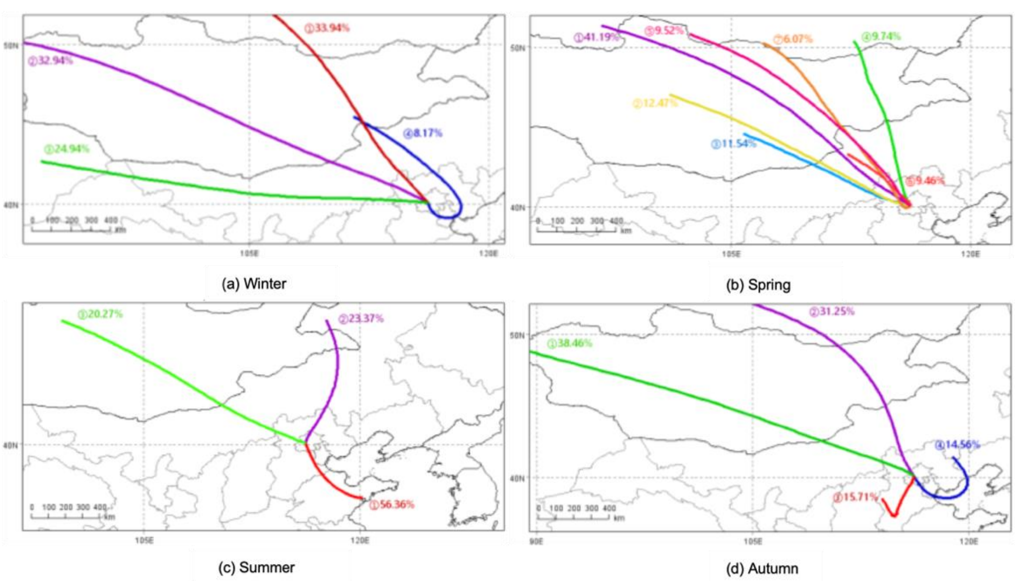

Figure 1. Backward trajectory clustering of airflow in four seasons in Beijing, China (2016 ~ 2021).

Table 1. Statistical Results of Particle Mass Concentration Corresponding to Various Air Streams in Four Seasons in Beijing

Season	Air mass type	Rate	$\rho^* / (\mu g \cdot m^{-3})$			$\rho^* / (\mu g \cdot m^{-3})$		
			$PM_{2.5}$	Std	Num	PM_{10}	Std	Num
Winter	1	33.94%	49.04	55.92	575	76.84	67.64	571
	2	32.94%	84.95	52.72	146	91.54	53.85	142
	3	24.94%	24.14	35.68	603	44.94	44.77	603
	4	8.17%	112.75	91.6	436	137.12	103.31	432
Spring	1	41.19%	41.42	50.44	757	101.68	178.94	747
	2	12.47%	85.44	47.54	211	116.88	52.12	204
	3	11.54%	18.57	16.66	176	47.2	38.12	176
	4	9.74%	77.98	53.8	227	121.45	77.68	220
	5	9.52%	41.72	19.79	111	81.92	48.88	109
	6	9.46%	69.58	52.51	172	86.19	52.04	161
	7	6.07%	36.26	27.9	174	104.25	123.74	164
Summer	1	56.36%	23.22	17.8	406	42.59	23.38	401
	2	23.37%	42.37	26.43	1019	58.74	32.27	997
	3	20.27%	27.18	20.55	360	52.61	36.64	358
Autumn	1	38.46%	18.16	17.63	553	40.96	35.08	547
	2	31.25%	47.81	34.95	251	65.61	39.68	248
	3	15.71%	40.8	40.96	693	71.22	58.9	686
	4	14.56%	78.67	47.76	278	98.72	45.74	274

and through Mongolia account for the highest proportion of the total airflow tracks this season, reaching 66.88%. The airflow track is long and the air mass moves fast. The airflow trajectory 3 coming from the Chinese Tian Shan Mountains and passing through the Inner Mongolia Plateau accounts for 24.94% of the airflow trajectory in this season. From the border between Mongolia and China, passing through Eastern Inner Mongolia and northeast Hebei in China, and circuitous westward to Beijing through Tianjin, the airflow trajectory 4 accounts for 8.17% of this season.

In spring, the airflow is mainly from north-central Mongolia, East and South Siberia in the northwest. Compared with the length of airflow in winter, the airflow in spring is relatively short and the movement speed of air mass is slow.

In summer, the airflow is mainly in the southeast direction, and the southeast direction (warm and humid airflow from the southeast ocean, track 1 passing through the east of Shandong Province and Hebei province) accounts for the largest proportion of the airflow in this season, accounting for 56.36%. The second is the airflow from Northeast Inner Mongolia province in the north, accounting for 23.37% of this season. The airflow from the northwest is shorter than that in winter and spring, and the proportion decreases, accounting for 20.27% of this season.

In autumn, the northwest airflow once again dominates. The airflow trajectory from Siberia (trajectories 1 and 2) is longer than that in summer, and the airflow moves faster and accounts for a larger proportion, accounting for about 69.71%. The airflow from the south of Hebei province (track 3) and the west of Bohai Sea (track 4) decreased in summer, accounting for 30.27% of this season.

3.2. Effects of Different Airflow Trajectories on Particle Concentration

Based on the cluster analysis results of the backward trajectory of airflow in each season in Beijing and combined with the particle concentration data, this study analyzes the impact of various trajectories on the atmospheric particulate matter in Beijing (Table 1).

In winter, the airflow from the junction of China and Mongolia (track 4) carries the highest concentrations of $PM_{2.5}$ and PM_{10}, which are 112.75 and 137.12 $\mu g \cdot m^{-3}$. The second is the long-distance transport flow from Siberia (track 2), with corresponding and average concentrations of 84.95 and 91.54 $\mu g \cdot m^{-3}$. The airflow path 4 passes through Tangshan and Qin Huangdao in Hebei Province, as well as Tianjin and other areas with developed heavy industry and dense population, and there are more polluting gases discharged during the heating period in winter, so the concentration of atmospheric particles carried by the airflow is high. Airflow trajectory 2 is long-dis-tance transportation with strong wind force and passes through the arid and semi-arid areas of Mongolia to transport a large amount of sand and dust to Beijing.

In spring, the average concentration of PM_{10} corresponding to the airflow from central and northern Mongolia (trajectories 1, 2, 4, and 7) is high, reaching 101.68, 116.88, 121.45, and 104.25 $\mu g \cdot m^{-3}$ respectively. Compared with winter, the trajectory distance of airflow from the northwest direction is shorter, but the concentration of particulate pollutants carried by the trajectory is significantly higher than that in winter.

In summer, the PM_{10} concentration corresponds to the airflow from the border between China and Mongolia, passing through Eastern Inner Mongolia Province and northern Hebei Province (track 2), and the airflow from central Mongolia (track 3) is higher, 58.74 and 52.61 $\mu g \cdot m^{-3}$. The PM_{10} concentration corresponding to the East Asian summer monsoon (track 1) passing through the Shandong Peninsula, Eastern Hebei Province, and Tianjin in China is 42.59 $\mu g \cdot m^{-3}$. Compared with other seasons, this season and the average concentration are the lowest, and the contribution of several airflow trajectories to the transport of air pollutant concentration in Beijing in summer is the same.

In autumn, the concentrations of $PM_{2.5}$ and PM_{10} corresponding to the airflow (track 4) from the junction of Meng-Ji-Liao through the Bohai Sea and Tianjin are the highest, 78.67 and 98.72 $\mu g \cdot m^{-3}$ respectively. The second is the airflow from East Belia through eastern Mongolia (track 2). The concentrations of $PM_{2.5}$ and PM_{10} are 47.81 and 65.61 $\mu g \cdot m^{-3}$ respectively, which indicates that these areas may transport atmospheric particles to Beijing in autumn.

To sum up, the northwest airflow from Siberia and central and Western Mongolia is the main long-distance transport route affecting the concentration of atmospheric particles in Beijing in four seasons. The southeast and northeast airflow passes through densely populated areas such as Hebei Province, Tianjin, and the Shandong Peninsula in China, with heavy pollution emission, making it another main transport route affecting the pollution of atmospheric particles in Beijing.

3.3. Analysis of Pollution Source Area

3.3.1. PSCF

The results of seasonal WPSCF of particulate matter in Beijing from 2016 to 2021 are shown in Figure 2. The color in the figure represents the contribution level of the potential source area. The darker the color, the greater the WPSCF value, and the greater the contribution of the area where the grid is located to the particulate matter mass concentration in Beijing.

The potential contribution source area of $PM_{2.5}$ in winter is affected by the northwest airflow and extends from the central part of Inner Mongolia to Beijing through Zhangjiakou. The high WPSCF value (> 0.3) is concentrated in Yanqing District, Changping District, Haidian District, Shijingshan District, Dongcheng District, Xicheng District, Fangshan District of Beijing, and the East of Baoding, and is distributed in blocks at the junction of Langfang and Tongzhou in Beijing and the west of Tianjin. In spring, the potential contribution source area of $PM_{2.5}$ moves southward, and the area with a high WPSCF value decreases, which is distributed in a belt from the south, middle, and north of Hebei to the south of Beijing. The WPSCF value of $PM_{2.5}$ in summer is the lowest in the four seasons, and the potential source area is the smallest. The potential source area is mainly distributed in the south of Hengshui, Baoding, and the northwest of Cangzhou. Affected by the marine airflow, there are also dotted low WPSCF value potential contribution source areas in the Shandong Peninsula, Bohai Sea, Tianjin, and other places. The range of potential contribution source areas of $PM_{2.5}$ in autumn is similar to that in spring. Most of them are distributed in central and Southern Hebei province, and there are few areas with high WPSCF value. They are dotted in the east of Shijiazhuang, the south of Baoding, the west of Langfang, and the junction of Daxing District, Fangshan District, Langfang, and Baoding. The mild potential contribution source areas are expanded compared with that in summer.

The distribution location and morphology of the potential contribution source area of PM_{10} in winter and spring are similar to that of $PM_{2.5}$. In winter, it is mainly the conveyor belt from central Inner Mongolia to Western Hebei to Beijing, and the higher WPSCF value (> 0.2) is dotted in Zhangjiakou, the junction of Yanqing District, and Huairou District, Fangshan District of Beijing, and the central and Western Tianjin; In spring, the WPSCF of potential contribution source areas dominated by central and Southern Hebei and Beijing is generally lower than 0.2. The potential contribution source area of PM_{10} in autumn is smaller than that in spring, and the WPSCF value is lower. It is distributed at the junction of Beijing and Baoding, Langfang, Tianjin, and the middle of Hebei province, and some are dotted at the junction of Hebei and Shandong. The WPSCF value of PM_{10} (0.05 < WPSCF< 0.25) is generally lower than that of $PM_{2.5}$ (0.1 < WPSCF < 0.4). This is because the main source of PM_{10} is soil, which is easy to settle, so the transmission distance of PM_{10} is relatively short, and the influence of PM_{10} will be reduced in the process of long-distance transportation.

In conclusion, the seasonal characteristics of WPSCF distribution of $PM_{2.5}$ and PM_{10} in Beijing are very obvious, and there are significant differences in the four seasons of potential contribution source areas. The high-value areas of WPSCF are the widest in winter, followed by spring, autumn, and summer. During the winter heating period, the main potential contribution sources of $PM_{2.5}$ and PM_{10} are concentrated in the West and south of Beijing and at the junction with Hebei and Tianjin due to the fine particles emitted by the combustion of fossil energy. In spring and autumn, affected by the airflow, most of the potential contribution source areas of $PM_{2.5}$ and PM_{10} are distributed in Shijiazhuang, Baoding, and other densely populated areas with frequent human activities in Hebei Province. Therefore, these places can be considered the main potential source areas in winter, spring, and autumn.

3.3.2. CWT

Because the potential source identified by the WPSCF method can only reflect the contribution rate of the potential source area, it can not extract the specific contribution level to the target grid. Therefore, the weighted calculation of pollutant mass concentration in the potential source grid according to the CWT can reflect the pollution degree of the potential source area.

The results show that the spatial distribution of potential pollution source areas of $PM_{2.5}$ and PM_{10} in the simulated four seasons is similar (Figure 3). In winter, the potential source areas of $PM_{2.5}$ and PM_{10} are dotted in central Inner Mongolia, banded in Zhangjiakou, Beijing, Langfang, the west of Tianjin, and the junction between Beijing and Baoding. The high WCWT value is mainly distributed in Beijing, the value of $PM_{2.5}$ is higher than 75 $\mu g \cdot m^{-3}$, and PM_{10} also has a high WCWT value (70 $\mu g \cdot m^{-3}$ < WCWT < 110 $\mu g \cdot m^{-3}$), which is related to the emission intensity of air pollutants during winter heating

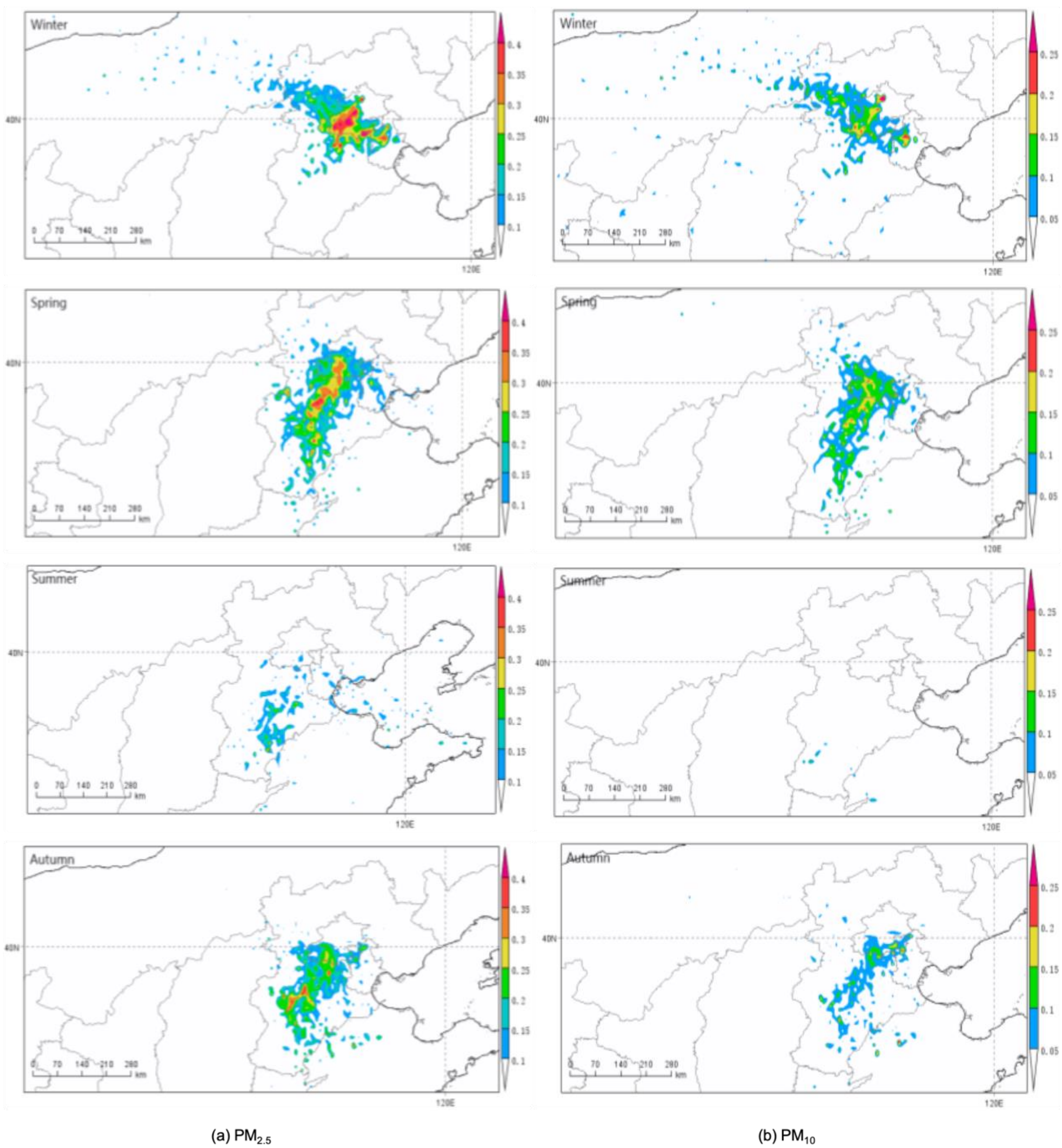

Figure 2. PSCF distribution of particulate matter in different seasons in Beijing, China.

period. The WCWT values of $PM_{2.5}$ and PM_{10} in spring are lower than 65 μg·m^{-3} and 110 μg·m^{-3} respectively. The higher WCWT values (55 μg·m^{-3} < WCWT < 65 μg·m^{-3}) are mainly distributed in the southwest of Beijing, the east of Baoding, and the west of Langfang. The distribution range of the source area tends to expand to the South and advance to the East. In summer, the WCWT values of $PM_{2.5}$ and PM_{10} are less than 45 and 70 μg·m^{-3} respectively. Their potential source areas are distributed in the south of Beijing, the east of Hebei province, Tianjin, the junction of Shandong and Hebei province, and the west of Bohai Sea. This distribution pattern is related to the prevailing marine monsoon flow in summer. The distribution of potential pollution source areas in autumn is similar to that in spring, but the distribution range of higher WCWT values is more scattered than that in spring, mainly at the junction of Beijing, Baoding, and Langfang, as well as the southwest of Baoding and the northeast of Shijiazhuang.

In conclusion, the seasonal distribution characteristics of WCWT of $PM_{2.5}$ and PM_{10} in Beijing are obvious, and there are significant differences in the four seasons of potential pollution source areas. The high-value areas of WCWT are the widest in winter, followed by spring, autumn, and summer. Therefore, Beijing, the west of Tianjin, the northeast of Baoding, the northwest of Langfang, the southwest of Baoding, and the northeast of Shijiazhuang are the main potential source areas of atmosphereic particulate matter.

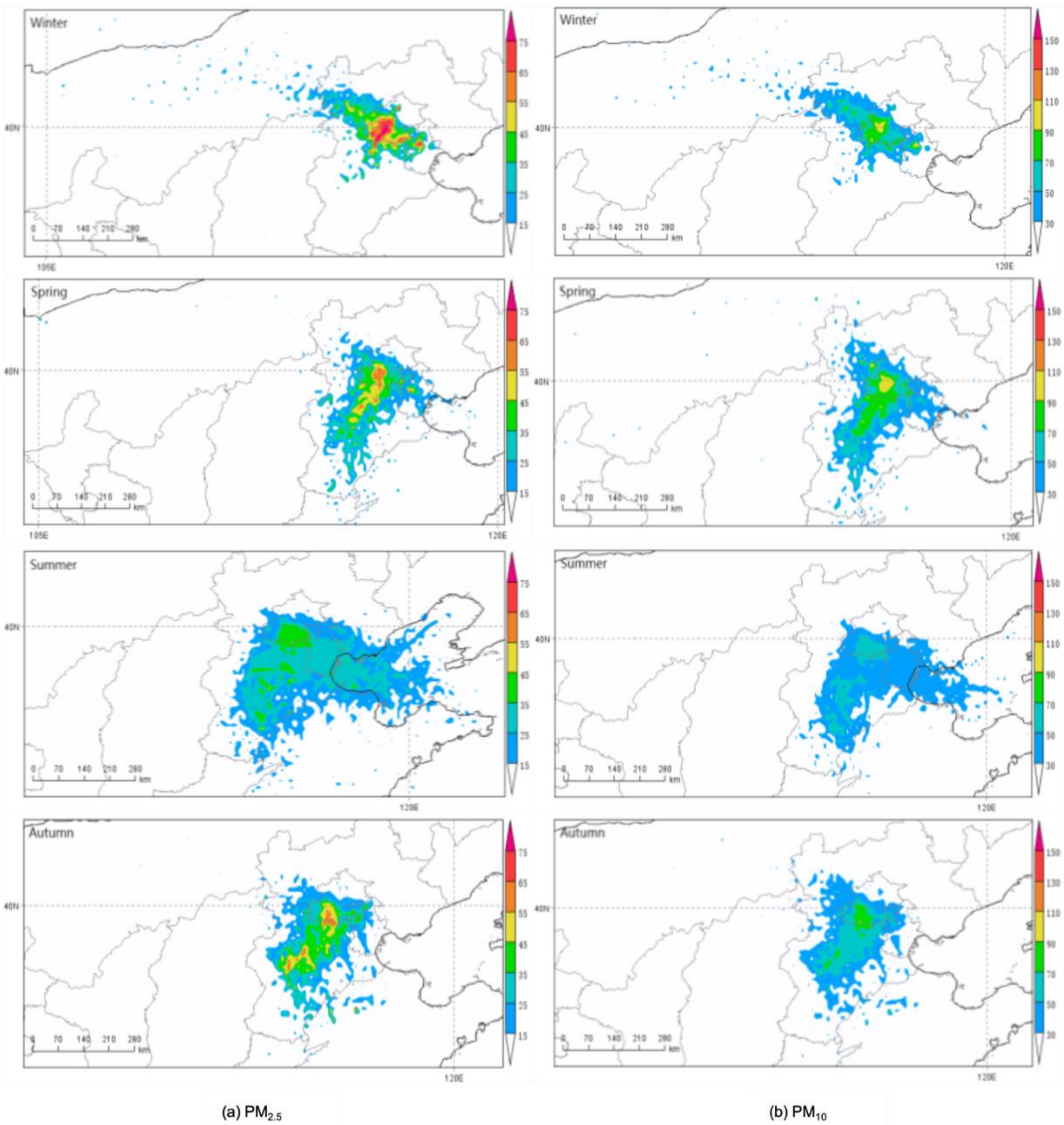

Figure 3. CWT distribution of particulate matter in different seasons in Beijing, China.

3.4. Correlation Analysis

In this part, the correlation effect of meteorological conditions in four seasons on the concentration of main air pollutants in Beijing is analyzed (Figure 4). The results show that the concentrations of $PM_{2.5}$ and PM_{10} in winter in Beijing have a strong positive correlation (corr > 0.6) with CO, SO_2, and nitrogen oxides (referred to by NO_2), and there is a strong negative correlation between the concentrations of these air pollutants and O_3 (corr < −0.54). For meteorological conditions, the concentrations of $PM_{2.5}$ and PM_{10} in winter have a positive correlation with relative humidity (RH), temperature (T), and cloud cover (Cloud), and a weak negative correlation with air pressure (SLP) and wind speed (Wind). The relative humidity and air temperature have the greatest impact on the concentration of $PM_{2.5}$ and PM_{10}, which indicates that under the conditions of high relative humidity, high temperature, thick clouds, low wind speed, and low air pressure, the concentration of atmospheric particulate matter is high, resulting in high AQI value and poor air quality. This meteorological condition slows down the movement speed of atmospheric particles and increases the sedimentation, which is easy to lead to heavy pollution. The correlation between the concentrations of $PM_{2.5}$ and PM_{10} in spring and other air pollutants and meteorological conditions is similar to that in winter, and both weaken to a certain extent, but the positive correlation with SO_2 concentration increases. Different from winter, spring, and autumn, O_3 concentration in summer has a strong positive correlation with $PM_{2.5}$ and PM_{10} concentration, and air pressure and temperature have a strong correlation with $PM_{2.5}$ and PM_{10} concentration compared with other meteorological factors. The negative correlation between atmospheric pressure and the concentrations of $PM_{2.5}$ and PM_{10} in autumn is stronger than that in spring, but the correlation between air temperature

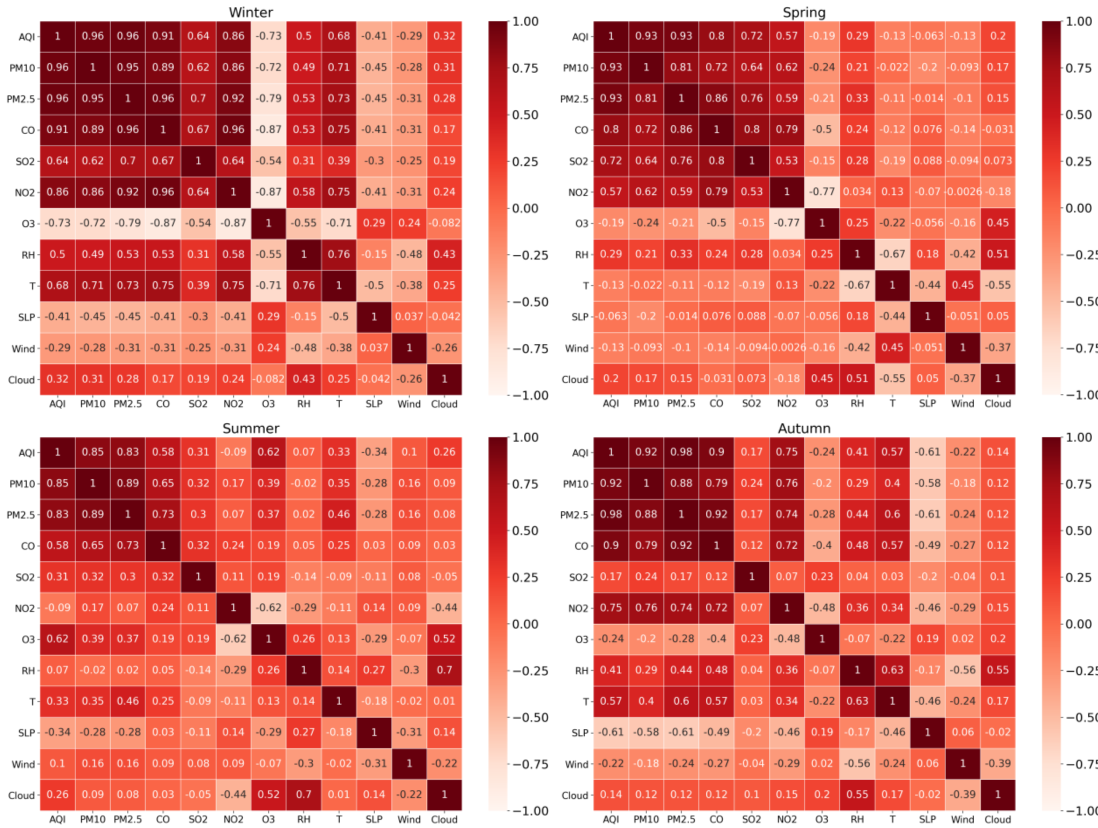

Figure 4. Correlation between pollutant concentration and meteorological factors in different seasons in Beijing.

is weaker than that in spring. Overall, air temperature and cloud thickness are always positively correlated with atmospheric particulate matter concentration, while air pressure and wind speed are always negatively correlated with atmospheric particulate matter concentration. The meteorological environment in different seasons has different effects on atmospheric particulate matter concentration.

4. Conclusions

(1) In summer, the monsoon flow from the southeast Ocean plays a leading role in Beijing, accounting for about 40%. In winter, spring, and autumn, the long-distance airflow in the northwest and biased towards the north are the main, and the proportion of the northwest airflow is the highest, which is higher than 60%, and the concentrations of $PM_{2.5}$ and PM_{10} in the northwest airflow track are higher than those of other airflows in the current season. These airflows come from or pass through the arid and semi-arid regions of the plateau such as the middle and west of Mongolia, passing through the Middle East of Inner Mongolia, and go eastward along Zhangjiakou to the Beijing plain. They are the main transport routes affecting the concentration of atmospheric particulate matter in winter, spring, and autumn in Beijing.

(2) Based on WPSCF, the potential source areas of $PM_{2.5}$ and PM_{10} in four seasons are spring, winter, autumn, and summer in turn. Based on WCWT, the weight potential source area of $PM_{2.5}$ and PM_{10} in four seasons is summer, autumn, spring, and winter. The results show that this distribution characteristic is directly related to the pollutant emission, meteorological conditions, and seasonal factors in the local and adjacent areas: The potential source areas of air pollutants in winter are mainly concentrated in Beijing and extend to the northwest, which is related to the combustion of a large amount of fossil energy in winter heating period. In spring and autumn, the potential source areas are mainly concentrated in central and southern Beijing and central and Southern Hebei province, and a small number of spots are distributed in Tianjin, Shandong province, and other places. In summer, the potential source area has a small range and low concentration, which is distributed in central and southern Beijing, central and Eastern Hebei province, Tianjin, Western Bohai Sea, and Northwest Shandong. Therefore, the pollution transport from North China and Huang Huai plain is the main contributing source of $PM_{2.5}$ and PM_{10} in the four seasons of Beijing urban area. It can be seen from the above that the pollution transportation from North China and Huang Huai plain is the main contributing source of $PM_{2.5}$ and PM_{10} in the four seasons of Beijing urban area. Therefore, the prevention and control of air pollution in Beijing should pay special attention to the short-distance transportation in the south of Beijing, the west of Tianjin, and the south of Hebei.

Since the mass concentrations of $PM_{2.5}$ and PM_{10} used in the potential source analysis in this study are the ground observation concentrations, which are different from the threedimensional spatial motion of the actual air mass, it can be considered to convert the mass concentrations of $PM_{2.5}$ and PM_{10} observed on the ground to the concentration at the starting height of the backward trajectory in the future. In addition, the follow-up research will further reduce the grid and time granularity, reduce the systematic error, and better analyze the temporal and spatial differences and evolution laws of the potential source areas of $PM_{2.5}$ and PM_{10} in Beijing, to provide a scientific basis for Beijing's atmospheric environment governance and regional emission reduction.

Acknowledgments. The $PM_{2.5}$ and PM_{10} datasets used in this study are available from the Beijing Municipal Econogical and Environmental Monitoring Center (http://beijingair.sinaapp.com/).

References

Ashbaugh, L.L., Malm, W.C. and Sadeh, W.Z. (1985). A residence time probability analysis of sulfur concentrations at grand Canyon National Park. *Atmospheric Environment*. 19(8), 1263-1270. https://doi.org/10.1016/0004-6981(85)90256-2

Balachandran, S., Chang, H. H., Pachon, J. E., Holmes, H. A., Mulholand, J. A. and Russell, A. G. (2013). Bayesian-based ensemble source apportionment of $PM_{2.5}$. *Environmental Science & Technology*. 47(23), 13511-13518. https://pubs.acs.org/doi/10.1021/es4020647

Borge, R., Lumbreras, J., Vardoulakis, S., Kassomenos, P. and Rodríguez, E. (2007) Analysis of long-range transport influences on urban PM_{10} using two-stage atmospheric trajectory clusters. *Atmosphereic Environment*. 41(21), 4434-4450. https://doi.org/10.1016/j.atmosenv.2007.01.053

Chen, Y.B., Xu, J., He, Y.J., Du, X.H., Tang, W. and Meng, F. (2016). Model analytic research of typical heavy PM2.5pollution periods in winter in Beijing. *Research on Environmental Sciences*. 29(5), 627-636. https://doi.org/10.13198/j.issn.1001-6929.2016.05.03

Draxler. R.R., Stunder, B., Rolph, G., Stein, A., Taylor, A., Zinn, S., Loughner, C. and Crawford, A. (2022). *HYSPLIT4 users guide [EB/OL].* NOAA Tech Mem Air Resources Laboratory. 02. https://www.ready.noaa.gov/hysplitusersguide/index.htm

Dimitriou, K. (2015). The dependence of PM size distribution from meteorology and local-regional contributions in Valencia (Spain) - A CWT model approach. *Aerosol and Air Quality Research*. 15(5), 1979-1989. https://doi.org/10.4209/aaqr.2015.03.0162

Do, W. G. and Jung, W. S. (2015). Estimation of PM10 source locations in Busan using PSCF model. *Journal of Environmental Science International.* 24(6): 793-806. https://doi.org/10.5322/JESI.2015. 24.6.793

Draxier, R.R. and Hess, G.D. (1998). An overview of the hysplit-4 modeling system for trajectories, dispersion and deposition. *Australian Meteorological Magazine*. 47(4), 295-308.

Du, P., Li, D.P., Liu, J.G., Zhang, J.S., Gui, H.Q., Yu, T.Z. and Wang, J. (2018). Pollution characteristics and potential source region analysis of atmospheric particulate matter during 2014 APEC in Beijing Surburban. *Acta Scientiae Circumstantiae*. 38(10), 3846-3855. https://doi.org/10.13671/j.hjkxxb.2018.0205

Geng, G.N., Zheng, Y.X., Zhang Q., Xue, T., Zhao, H.Y., Tong, D., Zheng, B., Li, M., Liu, F., Hong, C.P., He, K.P. and Davis, S.J. (2021). Drivers of PM2.5 air pollution deaths in China 2002-2017. *Nature Geoscience*. 14(9), 645-650. https://www.nature.com/articles/s41561-021-00792-3

Guo, X. N. and Ma, Y. C. (2020). Analysis of a typical heavy dust pollution weather in semi-arid region: A case study in eastern Qinghai. *EGU General Assembly 2020*. 41(2), 343-353. https://doi.org/10.5194/egusphere-egu2020-5220

Fu, C.B., Dan, L., Tang, J.X. and Tong, J.H. (2020). Analysis of air polluted transportation and potential source in Haikou City based on trajectory model. *Acta Scientiae Circumstantiae*. 40(1), 36-42. https://doi.org/10.13671/j.hjkxxb.2019.0244

He, L., Chen, H., Rangognio, J., Yahyaoui, A., Colin, P., Wang, J.H., Daële, V. and Mellouki, A. (2018). Fine particles at a background site in Central France: Chemical compositions seasonal variations and pollution events. *Science of the Total Environment*. 612, 1159-1170. https://doi.org/10.1016/j.scitotenv.2017.08.273

Liu, N., Ye Y., He J.J. and Zhao, S.P. (2013). Integrated modeling of urban-scale pollutant transport: Application in a Semi-arid Urban Valley, Northwestern China. *Atmospheric Pollution Research.* 4(3), 306-314. https://doi.org/10.5094/APR.2013.034

Li, X.S., Zhang, H., Yu, Y.Z., Deng, X.L., Luo, H.N., Zhang, J. and Xie, Q.W. (2022). Analysis of Potential Source Area of Air Pollution and Study on Transmission Channel in Chang-Zhu-Tan City Group during Intensive Care Period: Take Zhuzhou as an Example. *Environmental Monitoring and Forewarning*. 14(01), 19-27. https://doi.org/10.3969/j.issn.1674-6732.2022.01.004

Marcazzan, G. M., Vaccaro, S., Valli, G. and Vecchi, R. (2001). Characterisation of PM10 and PM2.5 particulate matter in the ambient air of Milan (Italy). *Atmospheric Environment*. 35(27), 4639-4650. https://doi.org/10.1016/S1352-2310(01)00124-8

Pey, J., Querol, X., Alastuey, A., Rodríguez, S., Putaud, J.P. and Dingenen, R.V. (2009). Source apportionment of urban fine and ultra-fine particle number concentration in a Western Mediterranean city. *Atmospheric Environment*. 43(29), 4407-4415. https://doi.org/10.1016/j.atmosenv.2009.05.024

Qian, W.M., Zhang, Y.P., Chen, J. and Han, J.C. (2018). Air pollutant transport channels and its potential sources in Shijiazhuang. *Acta Scientiae Circumstantiae*. 38(9), 3438-3448. https://doi.org/10.13671/j.hjkxxb.2018.0182

Salvador, P., Artinano, B., Pio, C., Afonso, J., Legrand, M., Puxbaum, H. and Hammer, S. (2010). Evaluation of aerosol sources at European high altitude background sites with trajectory statistical methods. *Atmospheric Environment*. 44 (19), 2316-2329. https://doi.org/10.1016/j.atmosenv.2010.03.042

Seibert, P., Kromp-Kolb, H., Baltensperger, U., Jost, D. T., Schwikowski, M., Kasper, A. and Puxbaum, H. (1994). Trajectory analysis of aerosol measurements at high alpine sites. *Academic Publishing*. 15(6): 689-693.

Stein, A.F., Draxler, R.R., Rolph, G.D., Stunder, B.J.B., Cohen, M.D. and Ngan, F. (2015). NOAA's HYSPLIT atmospheric transport and dispersion modeling system. *Bulletin of the American Meteorological Society*. 96 (12), 2059-2077. http://dx.doi.org/10.1175/BAMS-D-14-00110.1

Tian, M., Wang, H., Chen, Y., Yang, F.M., Zhang, X.H., Zou, Q., Zhang, R.Q., Ma, Y.L. and He, K.B. (2016). Characteristics of aerosol pollution during heavy haze events in Suzhou, China. *Atmospheric Chemistry and Physics*. 16(11), 7357-7371. http://dx.doi.org/10.5194/acp-16-7357-2016

Tiwari, S., Chate, D.M., Pragya, P., Ali, K. and Bisht, D.S. (2012). Variations in mass of PM10, PM2.5 and PM1 during the monsoon and the winter at New Delhi. *Aerosol and Air Quality Research*. 12, 20-29. https://doi.org/10.4209/aaqr.2011.06.0075

Tu, X.P., Yao, R.S., Gao, A.Z. and Shen, Y. (2019). Meteorological characteristics and outbreak causes of a heavy air pollution episode in northern Zhejiang Province. *Acta Scientiae Circumstantiae*. 39(5), 1443-1451. https://doi.org/10.13671/j.hjkxxb.2019.0032

Wang, X.Q., Lang, J.L., Cheng, S.Y., Chen, G.L. and Liu, X.Y. (2016). Study on transportation of $PM_{2.5}$ in Beijing-Tianjin-Hebei (BTH) and its surrounding area. *China Environmental Science*. 36(11), 3211-3217. https://doi.org/10.3969/j.issn.1000-6923.2016.11.002

Wang, F.L., Li, Z.Q., Yang, H., Wang, F.T., You, X.N., Zhang, M.J. Zhang, X. and Zhou, Q. (2020). Study on atmospheric particulate matter transport channel and pollution source area in Tianshui City. *Environmental Chemistry*. 39(9), 2371-2383. https://doi.org/10.7524/j.issn.0254-6108.2019061705

Wang, Y.Q., Zhang, X.Y. and Draxler, R.R. (2009). TrajStat: GIS-based software that uses various trajectory statistical analysis methods to identify potential sources from long-term air pollution measurement data. *Environmental Modelling & Software*. 24(8), 938-939. https://doi.org/10.1016/j.envsoft.2009.01.004

Yue, H.B., He, C.Y., Huang Q.X., Yin, D. and Bryan, B.A. (2020). Stronger policy required to substantially reduce deaths from PM2.5 pollution in China. *Nature Communications*. 11, 1462. https://doi.org/10.1038/s41467-020-15319-4

Zhang, J. R., Song, S. H., Xu, R. and Wen, J, H. (2017). Source of Airborne Particulate Matter in Guilin Based on Backward Trajectory Model. *Environmental Monitoring in China.* 33(2): 42-46. https://www.cnki.com.cn/Article/CJFDTotal-IAOB201702007.htm

Zhao, X.H., Tong, H.H., Wang, H.Y. and Geng, T.Z. (2020). Analysis of a typical pollution in autumn of Yangtze-Huaihe regions. *Environmental Monitoring in China*. 36(1), 34-44. https://doi.org/10.19316/j.issn.1002-6002.2020.01.05

Zheng, S.R., Kong, S.F., Yan, Q., Wu, J., Zheng, H., Cheng, Y., Yang, G.W., Wu, F.Q., Niu, Z.Z., Zeng, X., Li, F., Zheng, M.M., Chen, N., Xu, K., Yan, Y.Y. and Qi, S.H. (2019). Number concentration of submicron particles during winter at a suburban site of the south edge of North China. *China Environmental Science*. 39(11), 4511-4520. https://doi.org/10.19674/j.cnki.issn1000-6923.2019.0525

Zhu, B., Su, J.F., Han, Z.W., Yin, C., Wang, T. J. and Cai, Y. (2010). Analysis of a serious air pollution event resulting from crop residue burning over Nanjing and surrounding regions. *In Remote Sensing and Modeling of Ecosystem for Sustainability VII*. 7809, 80-85. https://doi.org/10.1117/12.860353